Pergamon

Engineering Fracture Mechanics Vol. 60, No. 1, pp. 47–58, 1998
© 1998 Elsevier Science Ltd. All rights reserved
Printed in Great Britain
PII: S0013-7944(97)00180-X 0013-7944/98 $19.00 + 0.00

EFFECT OF ARTIFICIAL CLOSURE MATERIALS ON CRACK GROWTH RETARDATION

P. S. SONG†
Department of General Courses, Chung Cheng Institute of Technology, Tahsi, Taoyuan 335, Taiwan, Republic of China

S. HWANG
Department of Civil Engineering, Chung Cheng Institute of Technology, Tahsi, Taoyuan 335, Taiwan, Republic of China

C. S. SHIN
Department of Mechanical Engineering, National Taiwan University, Taipei 106, Taiwan, Republic of China

Abstract—Premature crack closure plays a dominant role in affecting the crack driving force during fatigue. This work is focused on artificial infiltration of closure materials into a crack, promoting premature crack closure thereby depressing crack growth rate. Thus, service life is extended for cracked members. The test program was performed in 5083-O Al-alloy and AISI 4130 alloy steel, 9.8 and 3.6 mm in thickness, respectively. Pressurized nitrogen was utilized in boosting different closure materials into the crack. These materials include (i) epoxy resin modified with fine(0.05 μm) and coarse (1 μm) alumina powders, respectively; (ii) epoxy resin containing 1 μm silicon carbide powder; and (iii) silver paste. Experimental results indicated that, with the exception of silver paste, all the other closure materials work well in giving rise to different levels of crack closure and the accompanying growth retardation. The silicon carbide reinforced epoxy resin has the best retarding ability. The corresponding life extension exceeded 300 000 cycles. © 1998 Elsevier Science Ltd. All rights reserved

1. INTRODUCTION

IN THE field of fatigue, performing appropriate repair to fatigue-cracked structural components is one of the significant subjects, because requirements of economics increasingly demand greater extension of component operating life. To date, many crack repair techniques have been proposed for arresting or retarding crack propagation in structural components.

Under the material removal approach, the repair is to remove the damaged material to eliminate the surface cracks before its propagation to other area, thereby interrupting the failure mechanism, and a positive life gain is achieved [1]. In the case of deep-seated cracks, the application of this approach results in the over-removal of material and substantial loss of static and fatigue strength for the repaired body, inviting possible re-initiation of crack growth or overall catastrophic failure. Consequently, material removal approach is limited to shallow fatigue damage in thick-walled components. Repair welding is to reinforce the cracked body by depositing molten metal or weld material along the crack path. The molten material, when cool, acts as crack arrester, and reduces the driving force for crack propagation. Precaution is taken against the byproduct such as residual stresses, stress corrosion cracking, hydrogen embrittlement and so on [2]. In the case where the replacement or thorough repair is not convenient immediately upon crack discovery, drilling a stop hole at the crack tip may be a good first aid repair. A stop hole eliminates the sharp crack tip and the associated stress singularity [3–5]. Besides, the residual compressive stresses around the rim of the stop hole would delay the re-initiation of fatigue crack and depress the subsequent crack propagation. In practical application, however, it might not be possible to locate the crack tip precisely. Even if accurate location is achievable, this type of repair requires close inspection to ensure thorough removal of the crack tip. Moreover, the introduction of a stop hole is not applicable to pressure pipe lines, storage tanks

†Corresponding author. Tel: 00886 3 389 15 21; Fax: 00 886 3 389 15 19; e-mail: katze@cc04.ccit.edu.tw

and pressure vessels because it will lead to leakage. Steel balls or rollers may be impressed into the surface of a cracked component at both sides of the expected crack path, creating a region with residual compressive stresses between the impressions[5–8]. This, in turn, causes a delay in the crack growth, and the component fatigue life is extended. In practice, this type of repair works in the case of the through-thickness crack in the thin-walled components. Overloading an engineering component results in growth rate retardation and thus prolongs the fatigue crack growth life[9]. So far, an adequate method has not been available for adjusting the overload magnitude and applying it in due time for the purpose of extending the component life. Because small overload causes little delay, high overload may bring about catastrophic failure of the cracked body.

Since the pioneering work of Elber in the 1970s, which addressed closure behaviour for fatigue crack[10, 11], intensive attempts have been made to identify the crack closure mechanisms. These mechanisms include: (i) plasticity-induced closure [10, 11]; (ii) roughness of fracture surfaces[12]; (iii) phase transformation[13]; (iv) fracture surface oxidation[14]; and (v) viscous fluids penetrated inside the crack[15]. The understanding of these mechanisms unveils that most of the observed crack closure arises from the blockage caused by the ingress of excessive crack surface objects. Through this understanding, it occurred to the investigators that introducing artificially foreign objects into a crack might result in the premature crack closure and the subsequent crack retardation, and that use can be made of this concept in developing crack arresting methods. Shin and Hsu, trying the container-vaccumizing method in infiltrating the closure materials such as epoxy resin into the crack in the compact tension C(T) specimens, reported that premature crack closure occurs as expected and is accompanied by crack retardation[16]. Aqueous alumina infiltrant, epoxy resin and the mixture of epoxy resin were penetrated into the three-point bend specimens of AISI 304 stainless steel. Aqueous alumina infiltrant was ineffective in retarding crack growth, and the mixture of epoxy resin with 0.5 μm alumina showed satisfactory retardation performance[17, 18]. Upon these observations, the retardation effect of infiltrant properties warranted further investigation. Four types of closure materials were employed by UR-Rehman and Thomason[19]. Amongst these types of closure materials, the nickel-based materials did not show better retardation effect despite their superiority in hardness. This is because the nickel-covered crack surfaces were insignificant as well as at some distance from the crack tip. The increase in crack closure was, therefore, minor for growth retardation.

On the basis of the preceding discussion, the understanding is developed that crack growth retardation is artificially available through the infiltration of closure materials into a crack, and the infiltrant properties play a dominant role in promoting the crack closure and the retardation. To lay basis for further closure study, a test matrix was performed in the investigation of four closure materials with different degrees of hardness along with the specimens of an aluminum alloy and a low alloy steel. The closure materials include: (i) epoxy resin reinforced with alumina powder (0.05 and 1 μm in particle size); (ii) epoxy resin modified with silicon carbide powder (1 μm in particle size); and (iii) silver paste.

2. EXPERIMENTAL PROCEDURES

2.1. *Materials and test specimens*

The current test program was carried out on two test materials. These materials include 5083-O Al-alloy and AISI 4130 alloy steel. The chemical composition and mechanical properties of both materials are exhibited in Table 1.

Following the ASTM standard procedure E647-88a. Both of the test materials were machined into standard compact tension specimens of width 50.8 mm. The thickness was 9.8 mm with 5083-O Al-alloy specimens and 3.6 mm with AISI 4130 alloy steel specimens.

2.2. *Constant amplitude loading test*

All the experiments were conducted on a closed-loop electrohydraulic MTS system with a load capacity of 10 tons. The constant amplitude loading tests were performed at a cyclic fre-

Table 1. Chemical composition and mechanical properties of test materials

5083-O Al-alloy		AISI 4130 alloy steel	
Element	Wt(%)	Element	Wt(%)
Si	0.14	C	0.35
Fe	0.24	Mn	0.54
Cu	0.04	Si	0.23
Mn	0.59	Cr	1.03
Mg	4.43	Mo	0.22
Cr	0.10	–	–
Zn	0.05	–	–
Ti	0.01	–	–
Property	5083-O Al-alloy	AISI 4130 alloy steel	
Yield strength (MPa)	157	1170	
Tensile strength (MPa)	312	1380	
Young's modulus (GPa)	72	211	
Elongation (%)	25	16.5	

quency of 10 Hz and a stress ratio of $R = 0.1$. The crack was grown under constant amplitude loading of $\Delta P = 2835$ and 3150 N in 5083-O Al-alloy and AISI 4130 alloy steel, respectively. The crack length was monitored with a travelling microscope to a resolution of 0.01 mm. A back-face strain gage was used throughout the test for crack closure measurement. In defining the inflection point on the load–displacement curve that best quantifies the opening level, the offset procedure, which is similar to that employed by Shin and Hsu[20], was utilized. The loading frequency was decreased to 0.05 Hz during the closure measurement in preventing a low signal to noise ratio from providing misleading information on crack closure. The magnitude of the crack closure is quantified in terms of the fraction U.

$$U = \frac{K_{max} - K_{op}}{K_{max} - K_{min}} = \frac{\Delta K_{eff}}{\Delta K}, \tag{1}$$

where K_{max}, K_{min}, are the maximum and minimum applied stress intensity, and K_{op} is the stress intensity at which the crack starts to become fully open.

2.3. *Crack-filling closure test*

The crack-filling closure test was run at a stress ratio of $R = 0.1$ along with the stress intensity factor range ΔK of 8 and 26 MPa $\sqrt{m}$ in 5083-O Al-alloy and AISI 4130 alloy steel, respectively. Load shedding was done manually in order to maintain a constant ΔK condition during the baseline loading. With the crack propagation at a predetermined crack size, at which the steady-state was established for certain with crack growth rate and closure behaviour, the normal fatigue loading was interrupted and a static load of $0.95K_{max}$ was applied to open the crack for the insertion of a tungsten carbide wedge. During the insertion process, the signals from the back-face strain gage were monitored continuously using a strain indicator in keeping the observed strain below that corresponding to the current K_{max}. After the insertion, the specimen is unloaded, and the wedge is held in place within the crack with the restoration of specimen elasticity to pre-insertion level. The specimen containing the wedge is removed from the fatigue machine for the infiltration of closure materials into the crack. The closure materials and infiltration technique are detailed in the next section. The fatigue test was continued after the completion of the infiltration process. The crack closure measurement was performed more often over the immediately-after-infiltration period than over the normal period, during which the closure measurement was performed every 0.5 mm of crack increment.

2.4. *Closure materials and infiltration technique*

The basic ingredient of the current closure materials is epoxy resin. Epoxy resin has advantages including: (i) adhesive, but non-corrosive to metal surfaces; (ii) non-volatile with negligible volume change during hardening process; and (iii) good resistance to weathering action as well as chemical attack. In enabling insight toward the hardness effect of closure materials on crack

Table 2. The test materials and the closure-material mixes

Type of test material	Type of closure material	Average particle size of powdered additive (μm)	Epoxy resin: powdered additive (by weight)
5083-O Al-alloy	Alumina powder modified epoxy resin	0.05	2:1
		1.0	2:1
	Silicon carbide powder reinforced epoxy resin	1.0	2:1
	Silver paste	–	–
AISI 4130 alloy steel	Alumina powder modified epoxy resin	0.05	2:1
		1.0	2:1
	Silicon carbide powder reinforced epoxy resin	1.0	2:1

closure, epoxy resin is modified with fine (0.05 μm) and coarse (1 μm) alumina powders as well as with 1 μm silicon carbide powder. In contrast to the hard epoxy resin, a soft silver paste has also been used. The proportions of the ingredients are listed in Table 2 for the current closure materials. In addition to the strength of the closure materials, the dependence of crack closure effect on successful penetration of infiltrant is substantially strong. To achieve good penetration, the pressurized nitrogen method was employed. The infiltration technique is performed as follows. The crack path was encircled by a hollow rubber bung on either surface of the specimen. The bung was connected through plastic tubing to a nitrogen bottle, after application of the infiltrant along the crack path. The along-crack-path infiltrant was forced thicknesswise through the specimen. The infiltration process was completed after the infiltrant showed up on the opposing specimen surface. The specimen was allowed to stand still in room temperature air for about 24 h till the infiltrant was dry with full development of hardness. After this, the tungsten carbide wedge was removed and the fatigue test was continued.

3. RESULTS AND DISCUSSION

Following the baseline data on the present constant amplitude loading test, the dependence of crack growth rate da/dN on the applied stress intensity range ΔK is given according to the Paris relation as follows:

$$\frac{da}{dN} = 8.73 \times 10^{-9}(\Delta K)^{4.17} \text{ for } 5083 - \text{O Al} - \text{alloy}, \tag{2}$$

$$\frac{da}{dN} = 2.12 \times 10^{-9}(\Delta K)^{3.15} \text{ for AISI 4130 alloy steel}, \tag{3}$$

where the unit of da/dN is mm/cycle and that of ΔK is MPa $\sqrt{m}$. To take account of the closure effect in accordance with Elber's modification to the Paris relation, eqs (2) and (3) are modified as:

$$\frac{da}{dN} = 1.01 \times 10^{-8}(\Delta K_{\text{eff}})^{4.31} \text{ for } 5083 - \text{O Al} - \text{alloy} \tag{4}$$

and

$$\frac{da}{dN} = 5.34 \times 10^{-9}(\Delta K_{\text{eff}})^{2.97} \text{ for AISI 4130 alloy steel}. \tag{5}$$

With information available on the applied ΔK and the crack closure value, crack growth rate in 5083-O Al-alloy and AISI 4130 alloy steel may be calculated using eqs (4) and (5), respectively.

The relation between the crack length and loading cycles is shown in Fig. 1 with 5083-O specimen tested in the presence of 0.05 μm alumina reinforced epoxy resin. The slope of the a–N curve remains constant prior to the infiltration process, suggesting a constant growth rate. Pronounced slope-change is observed with infiltration at crack size of 15.12 mm shown by the arrow. The post-infiltration retardation persists over about 250 000 cycles. The amount of life extension may be deduced by extrapolating the initial constant growth rate portion and comparing it with the currently observed a–N curve. The resulting life extension so deduced was 172 000 cycles. The insight into the infiltration-induced retardation is available in the crack

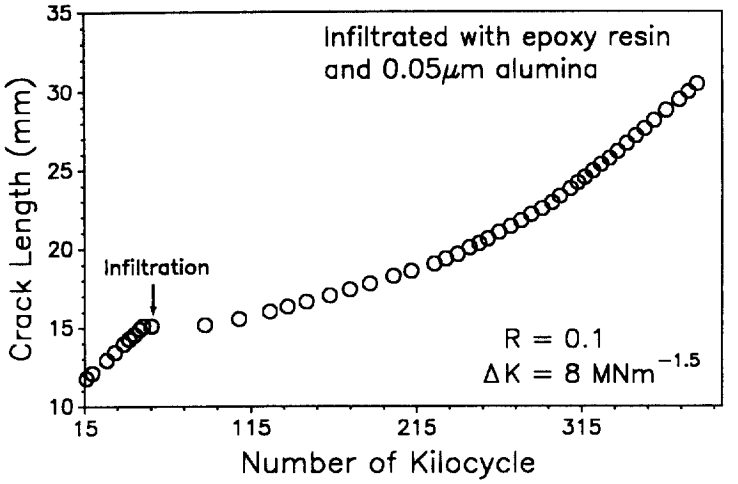

Fig. 1. Crack length against fatigue cycles relationship of 5083-O specimen infiltrated with 0.05 μm alumina reinforced epoxy resin.

growth rate against crack length curve shown in Fig. 2 (open circle). Prior to the infiltration, the steady-state is established with the crack propagating at the rate of approximately 9.8×10^{-5} mm/cycle. On resuming the test after the infiltration process, the crack growth rate falls steeply and immediately to $\sim 2.0 \times 10^{-6}$ mm/cycle. The delay ratio, D, of the minimum to the baseline growth rate is as low as 0.02. The marked post-infiltration drop in the crack growth rate indicates that filling the crack with closure material has a fair effect on the reduction in the crack-tip stress intensity, and thus retards the crack growth rate. Immediately after approaching a minimum, the growth rate gradually increases and recovers to the pre-infiltration level. The infiltration-induced retardation persists over a growth interval of about 11.88 mm. The predicted crack growth rate based on Paris relation taking into account the measured U values (shown in Fig. 3) is also illustrated in Fig. 2 (filled circle). The predicted growth rate correlates with the observed growth rate before infiltration. The minimum predicted rate after infiltration is about 2.8×10^{-7} mm/cycle, which is lower than the minimum observed rate. After the infiltration, the predicted growth rate stays below the observed growth rate till the pre-infiltration rate is achieved. The difference between measured and predicted crack growth rate is probably the result of discontinuous closure phenomenon[21]. This phenomenon results in because the closure wedge did not reach as far as the crack tip. Upon unloading, the closure instrumentation will be

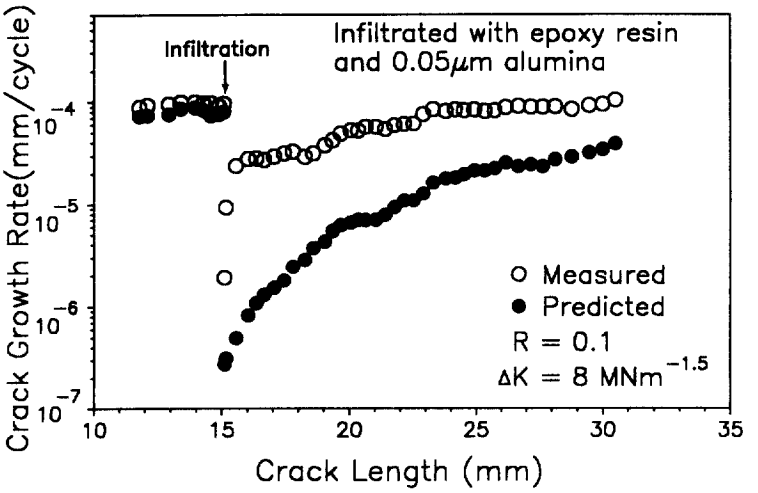

Fig. 2. Variation of fatigue crack growth rate with crack length of 5083-O specimen in the presence of 0.05 μm alumina reinforced epoxy resin.

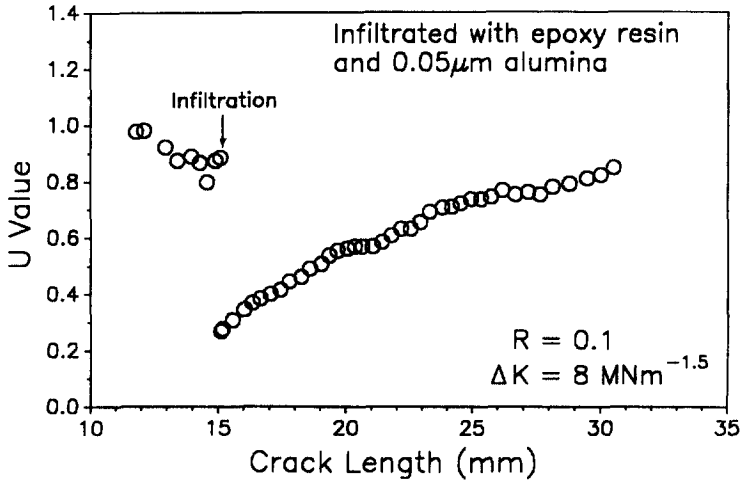

Fig. 3. Measured closure level against crack length relationship with 5083-O specimen containing 0.05 μm alumina reinforced epoxy resin.

triggered when the wedge starts to come into contact with the fracture surface, yet the crack tip still remained open. The closure instrumentation will record an U value smaller than is actually seen by the crack tip, leading to an underestimation of the growth rate using eq. (4). Figure 3 shows the throughout-test development of crack closure. The value of U is kept constant at about 0.9 before the infiltration process and catches up with the pre-infiltration value gradually after decaying to the minimum value of $U_{min} = 0.27$.

The loading cycles dependence on crack length is given in Fig. 4 with the AISI 4130 alloy steel specimen tested in the presence of epoxy resin containing 0.05 μm alumina. A substantial change is observed in the slope of the crack length against loading cycles curve with the infiltration process conducted at a crack size of 15.92 mm. The gain in fatigue life is up to 209 000 cycles. The corresponding variation in U value is shown in Fig. 5 with the sharp drop to the value of $U_{min} = 0.35$ following the crack penetration of closure material. Figure 6 shows the measured and predicted growth trends with AISI 4130 alloy steel specimen tested in the presence of epoxy resin containing 0.05 μm alumina. Similitude exists between Figs 2 and 6. The measured crack growth rate decreases from the pre-infiltration level of about 5.6×10^{-5} mm/cycle to the post-infiltration level of $\sim 2.8 \times 10^{-6}$ mm/cycle. The ratio of the minimum to the baseline growth rate is 0.05 and the infiltration-affected crack length is about 12.29 mm.

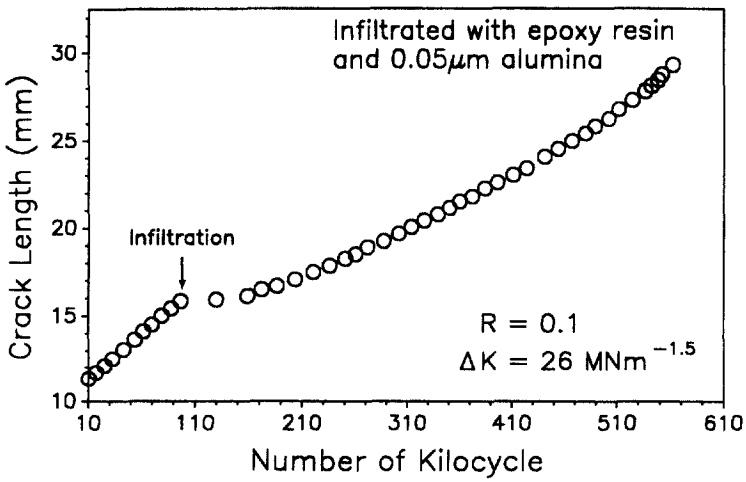

Fig. 4. Crack length against fatigue cycles relationship of AISI 4130 specimen infiltrated with 0.05 μm alumina reinforced epoxy resin.

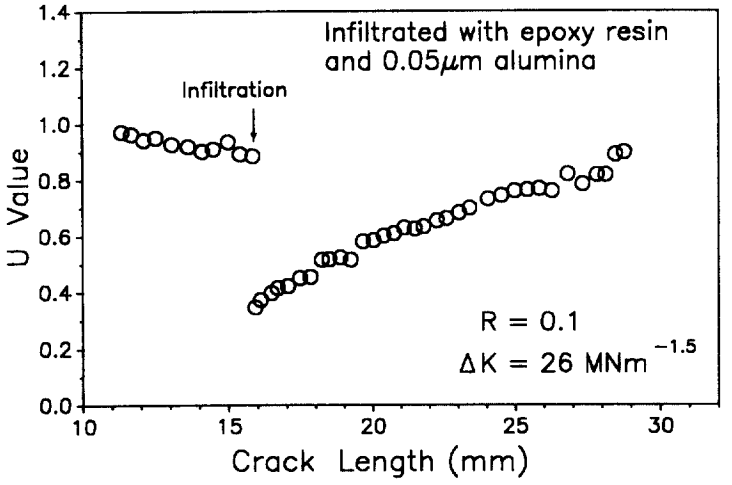

Fig. 5. Crack closure development for AISI 4130 specimen containing 0.05 μm alumina reinforced epoxy resin.

Additionally, the comparisons between the predicted and the measured crack growth rates made in Figs 2 and 6, respectively, indicate that the underestimate of cracking rate is more marked in 5083-O Al-alloy than in AISI 4130 alloy steel. Leaving aside the lower U_{min} value for the post-infiltration growth in 5083-O Al-alloy, this underestimate probably arises from the test parameters and the material properties adopted in the present study. The stress intensity factor range ΔK is taken at 8 and 26 MPa $\sqrt{m}$ for 5083-O Al-alloy and AISI 4130 alloy steel, respectively. The yield strength σ_y is 157 and 1170 MPa with the former and latter materials, respectively. The crack-tip plastic zone is much larger in 5083-O Al-alloy than in AISI 4130 alloy steel, considering the fact that the plastic zone size is proportional to the quantity $(\Delta K/\sigma_y)^2$. As the crack advances through the crack-tip plastic zone, the free surface protrudes toward the fracture surface in the plastic wake, subjected to the residual compressive stress exerted by the surrounding material. The amount of the protrusion is probably greater in 5083-O Al-alloy than in AISI 4130 alloy steel and, as result, the closure effect is stronger in the former test material than in the latter. Thereby, the predicted growth trend lies far below the observed trend for 5083-O Al-alloy than for AISI 4130 alloy steel.

Shown in Fig. 7 is the crack length versus loading cycles curve with 5083-O Al-alloy specimen containing silver paste. A minor drop in the slope for the curve is observed following the

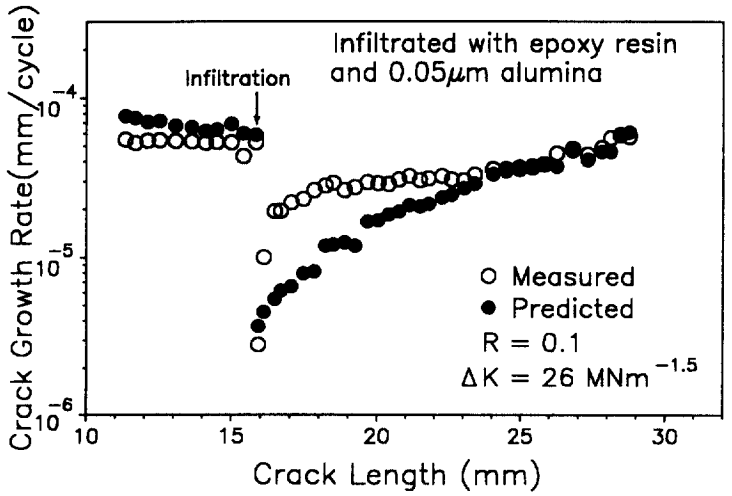

Fig. 6. Comparison between predicted and measured crack growth rates for AISI 4130 specimen in the presence of 0.05 μm alumina reinforced epoxy resin.

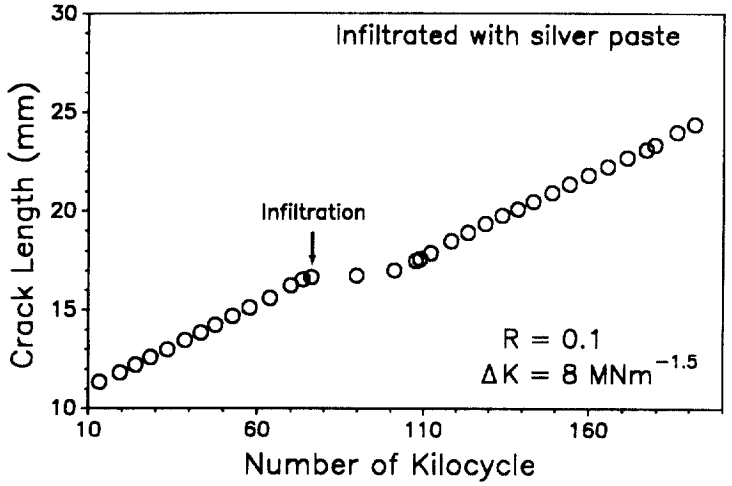

Fig. 7. Loading cycles dependence of crack length in 5083-O specimen infiltrated with silver paste.

infiltration process conducted at a crack size of 16.53 mm, and the recovery of the growth rate to the pre-infiltration level is achieved within a few loading cycles. The fatigue-life gain is just roughly 23 000 cycles. The corresponding behaviour of U is plotted in Fig. 8 throughout the test with the value of $U_{min} = 0.42$, slightly higher than those with other closure materials as Table 3 suggests. The slightly higher value of U_{min} gives an indication of poor closure effect along with attenuated retardation. In fact, the observation made with the travelling microscope throughout the test period shows that silver paste was squeezed out of the growing crack easily with the closure effect minimized no sooner than the fatigue test was continued. This observation arises from that fact that silver paste is the softest of the current closure materials with poor resistance to the action of the repeated loads and, therefore, is the least capable of carrying the loads transmitted between the crack surfaces. Due to the poor effectiveness in inducing crack closure and subsequent growth retardation, use is not made of silver paste any more in tests conducted on AISI 4130 alloy steel. The effects of present closure materials on growth retardation are shown in Table 3. The tabulated data demonstrate that, apart from the silver paste, all of the current closure materials have retarding effects of various degrees on the crack growth in both test materials. In enabling an insight into the hardness effect of the present closure materials on crack closure and the accompanying crack retardation, the hardness test was conducted using

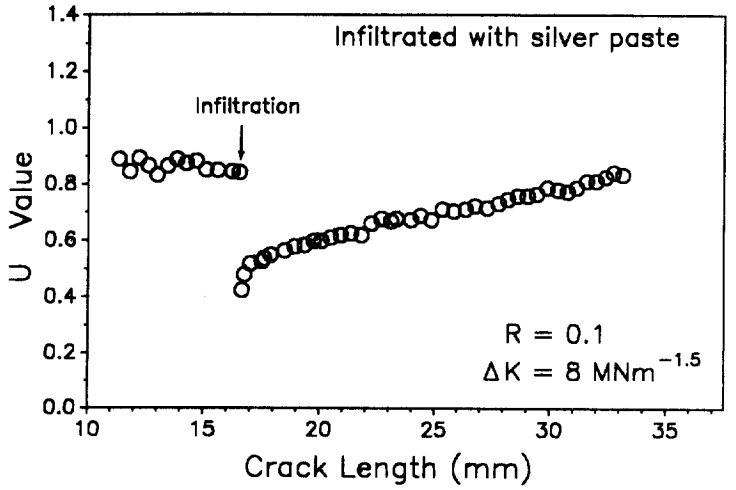

Fig. 8. The relationship between closure level and crack length with 5083-O specimen infiltrated with silver paste.

Table 3. Artificial-retardation related growth data

Type of test material	Type of closure material	U_{min}	D^a	Infiltration-affected crack length (mm)	life extension (No. of cycles)	Rockwell superficial hardness value
5083-O Al-alloy	0.05 μm alumina reinforced epoxy resin	0.27	0.02	11.88	172 000	15W25
	1 μm alumina reinforced epoxy resin	0.15	0.01	15.20	231 000	15W27
	1 μm silicon carbide reinforced epoxy resin	0.36	0.08	13.96	301 000	15W51
	Silver paste	0.42	0.15	0.96	23 000	[b]
AISI 4130 alloy steel	0.05 μm alumina reinforced epoxy resin	0.35	0.05	12.29	209 000	15W25
	1 μm alumina reinforced epoxy resin	0.33	0.06	11.71	202 000	15W27
	1 μm silicon carbide reinforced epoxy resin	0.39	0.08	11.89	304 000	15W51

[a] D denotes the ratio of the minimum to the baseline growth rate.
[b] Too soft to produce sensible reading.

the Rockwell superficial hardness tester. Silver paste has hardness beyond the lower bound of Rockwell superficial hardness range. The epoxy resin has Rockwell hardness values of 15W27 and 15W25, being reinforced with 1 and 0.05 μm alumina, respectively. The Rockwell hardness value is up to 15W51 for epoxy resin modified with 1 μm silicon carbide. The examination of retardation data, along with the hardness values, indicates that the epoxy resin containing silicon carbide has a stronger retarding effect on crack growth and the corresponding life extension exceeds 300 000 cycles for both test materials, being greater than the life extension with other closure materials. This probably implies that the harder closure material has a stronger retarding effect on crack growth, because the harder the material, the more capable it is of carrying the loads transmitted between the fracture surfaces. Thus, a greater reduction in ΔK_{eff} is yielded and a stronger retardation effect arises. Alternatively, understanding is developed of hardness effect

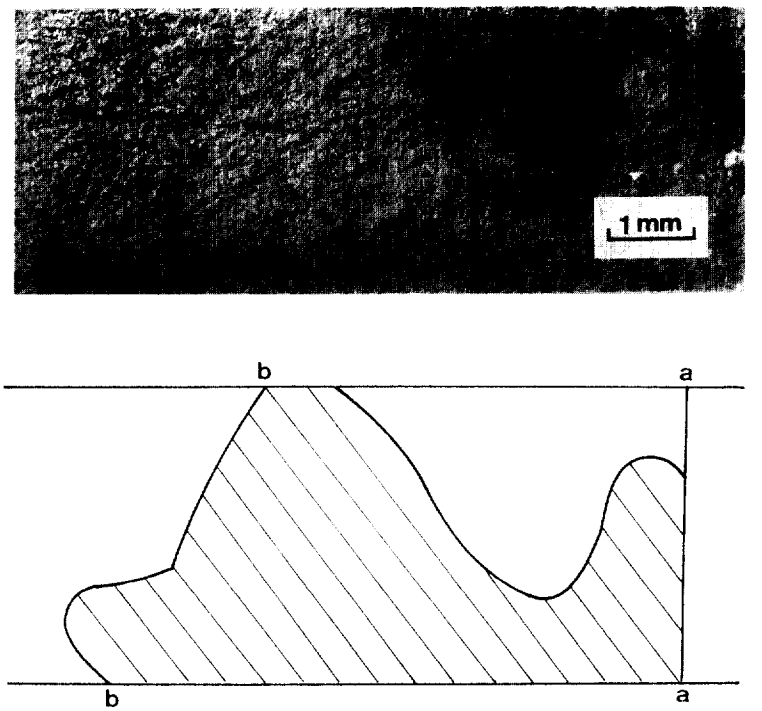

Fig. 9. Fractograph of the fracture surface of the AISI 4130 specimen covered with epoxy resin modified with 1 μm silicon carbide.

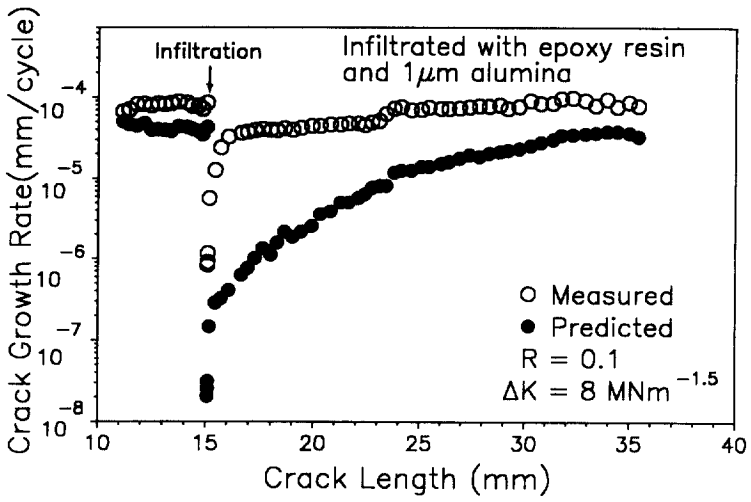

Fig. 10. Measured and predicted crack growth rates with the presence in 5083-O specimen of 1 μm alumina reinforced epoxy resin.

on crack retardation through the infiltration associated U_{min} value for the current closure materials. The lower value for U_{min} indicates that greater reduction in crack growth rate is achieved with closure materials, and that a longer period of crack growth is necessary for the pre-infiltration growth rate to be caught up, i.e. the life extension is greater. In the case of fatigue tests on 5083-O Al-alloy, U_{min} has values of 0.27 and 0.15 for epoxy resin modified with 0.05 and 1 μm alumina, respectively, with a slight difference in hardness between these two closure materials, and the life extension is greater for the latter closure material than for the former, consistent with the preceding U_{min} argument. In contrast, considerable increase was still observed in life extension, while U_{min} was as high as 0.36 when 5083-O specimen was tested with silicon carbide reinforced epoxy resin. The greater hardness with silicon carbide probably contributed to this increase in life extension. Similar observation was made on AISI 4130 alloy steel specimen containing epoxy resin reinforced by silicon carbide. In this case, U_{min} has a value up to 0.39, higher than those for other closure materials, and the corresponding life extension is greater than those with other closure materials by about 100 000 cycles.

Table 3 also provides implicitly the information concerning the infiltration ability of current infiltration technique. A slight difference in the life extension is observed between 5083-O Al-alloy and AISI 4130 alloy steel specimens with the identical closure material, even though the

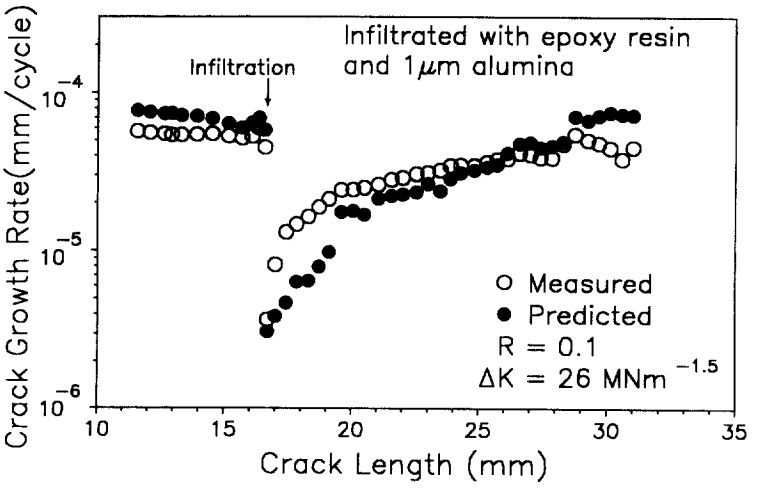

Fig. 11. Comparison between predicted and observed crack growth rates for AISI 4130 specimen infiltrated with 1 μm alumina reinforced epoxy resin.

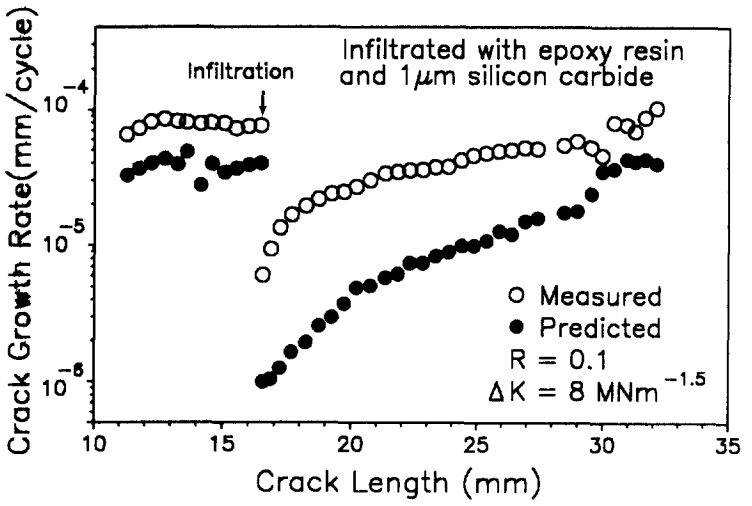

Fig. 12. Measured and predicted crack growth rates with the presence in 5083-O specimen of 1 μm silicon carbide modified epoxy resin.

5083-O Al-alloy specimen is 2.7 times greater than AISI 4130 alloy steel specimen in thickness. The current infiltration technique is, therefore, somewhat independent of the specimen thickness.

Figure 9 shows the extent and distribution of epoxy resin reinforced by 1 μm silicon carbide on the fracture surface of AISI 4130 alloy steel specimen. Line a–a indicates the notch position, line b–b the boundary of closure material covered area and shaded area the closure-material covered region. It is observed fractographically that the considerable portion of the crack surface is covered with the closure material.

Shown in Figs 10 and 11 are the comparisons between the observed and the predicted crack growth rates with both 5083-O Al-alloy and AISI 4130 alloy steel specimens tested in the presence of epoxy resin containing 1 μm alumina, respectively. It is appreciated that, as result of discontinuous closure[21], the predicted growth trends lie below the observed trends. Figures 12 and 13 give the relationships between the observed and predicted crack growth rates with 5083-O Al-alloy and AISI 4130 alloy steel specimens tested in the presence of epoxy resin containing 1 μm silicon carbide, respectively. The growth trends are similar to those shown in Figs 10 and 11. The growth rate falls to a minimum immediately after infiltration, followed by a gradual

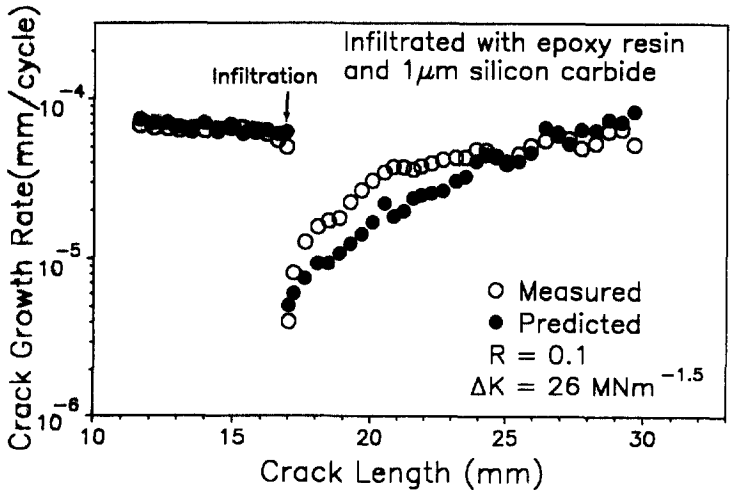

Fig. 13. Comparison between predicted and observed crack growth rates for AISI 4130 specimen infiltrated with 1 μm silicon carbide modified epoxy resin.

return to the pre-infiltration cracking rate within a period of certain crack length. Understanding is developed that closure materials penetrated inside the crack significantly increase retardation effect.

4. CONCLUDING REMARKS

The current crack-retarding method lies in the introduction of foreign objects into a crack for the promotion of premature crack closure and, therefore, growth retardation. Pressurized nitrogen is useful in forcing the closure materials into the crack. Epoxy resin was chosen as the predominant constituent of the present closure materials in that good adhesiveness promises enhancement of the closure effect with less scaling from the crack surfaces under repeated actions of the loads transmitted between the crack surfaces. The epoxy resin base closure material contributes to the infiltration induced crack retardation and the silicon carbide reinforced epoxy resin exhibits better retarding effect with greater hardness. Futher effort is suggested on the upgrade of the current method for life extension in cracked components.

REFERENCES

1. Popp, H. G., Wilbers, L. G. and Erdeman, V. J., Fatigue damage and repair of jet engine components. *ASTM STP*, 1971, **495**, 228–253.
2. Linnert, G. E., *Welding Metallurgy*, Vol.2. American Welding Society, New York, 1967.
3. Broek, D., *Elementary Engineering Fracture Mechanics*, 4th edn. Martinus Nijhoff, The Hague, 1986.
4. de Rijk, P., Empirical investigation on some methods for stopping the growth of fatigue crack. Nat. Aerospace Inst. Amsterdam, Report TR 70021, 1970.
5. van Leeuwen, H. P. *et al.*, The repair of fatigue cracks in low-alloy steel sheet. Nat. Aerospace Inst. Amsterdam Report TR 70029, 1970.
6. Eggwirtx, S., Review of some Swedish investigations on fatigue during the period 1967–1969. Swedish Aerospace Inst. FFA Report TN-HE-1270, 1969.
7. Blazewicz, W., Results reported in Schijve, J., lecture II—fatigue cracks, plasticity effects and crack closure. *Engng Fract. Mech.*, 1979, **11**, 182–196.
8. Landy, M. A., Armen, H. Jr and Eidinoff, H. L., Enhanced stop-drill repair procedure for cracked structures. *ASTM STP*, 1986, **927**, 190–220.
9. Novotny, L. G., Overstressing of pressure vessels to increase service life. *Proc. Inst. Mech. Engrs U.K.*, 1986, **C268/86**, 249–256.
10. Elber, W., Fatigue crack closure under cyclic tension. *Engng Fract. Mech.*, 1970, **2**, 37–45.
11. Elber, W., The significance of fatigue crack closure. *ASTM STP*, 1971, **486**, 230–242.
12. Halliday, M. D. and Beevers, C. J., Non-closure of crack and fatigue crack growth in β-heat treated Ti-6Al-4V. *Int. J. Fract.*, 1979, **15**, 27–30.
13. Pineau, A. G. and Pelloux, R. M., Influence of strain-induced martensitic transformations on fatigue crack growth rates in stainless steels. *Metall. Trans.*, 1974, **5A**, 1103–1112.
14. Suresh, S. and Ritchie, R. O., On the influence of environment on the load ratio dependence of fatigue thresholds in pressure vessel steel. *Engng Fract. Mech.*, 1983, **18**, 785–800.
15. Tzou, J. L., Suresh, S. and Ritchie, R. O., Fatigue crack propagation in oil environments—I. Crack growth behavior in silicone and paraffin oils. *Acta Metall.*, 1985, **33**, 105–116.
16. Shin, C. S. and Hsu, S. H., Fatigue life extension by an artificially induced retardation mechanism. *Engng Fract. Mech.*, 1992, **43**, 677–684.
17. Sheu, B. C., Song, P. S. and Shin, C. S., The effect of infiltration induced crack closure on crack growth retardation. *Scripta Metall.*, 1994, **31**, 1301–1306.
18. Shin, C. S., Wang, C. M. and Song, P. S., Fatigue damage repair: a comparison of some possible methods. *Int. J. Fatigue*, 1996, **18**, 535–546.
19. UR-Rehman, A. and Thomason, P. F., The effect of artificial fatigue-crack closure on fatigue-crack growth. *Fatigue Fract. Engng Mater. Struct.*, 1993, **16**, 1081–1090.
20. Shin, C. S. and Hsu, S. H., On the mechanisms and behaviour of overload retardation in AISI 304 stainless steel. *Int. J. Fatigue*, 1993, **15**, 181–192.
21. Brahma, K. K., Dash, P. K. and Dattaguru, B., Observation of crack closure using a crack mouth opening displacement gauge. *Int. J. Fatigue*, 1989, **11**, 37–41.

(*Received* 1 *November* 1996, *in final form* 17 *October* 1997, *accepted* 28 *November* 1997)